

Research Paper

Mapping Sound Pressure Levels: A Novel Approach to Determining Near-field and Far-field Regions

Iliyan Yordanov ILIEV^{(1)*}, Hristo Zhivomirov KARAIIVANOV⁽²⁾⁽¹⁾ *Department of Information Technology, Nikola Vaptsarov Naval Academy
Varna, Bulgaria*⁽²⁾ *Department of Theory of Electrical Engineering and Measurements, Technical University of Varna
Varna, Bulgaria**Corresponding Author e-mail: i.y.iliev@naval-acad.bg*(received May 30, 2024; accepted February 5, 2025; published online April 2, 2025)*

The present study focuses on the spatial characteristics of the sound pressure level (SPL) generated by a circular piston (a circular-shaped acoustic transducer or loudspeaker). It presents a short theoretical review to aid understanding the primary sound field characteristic – acoustic pressure – as a function of time, frequency, directivity angle, and distance from the source. The study introduces a simple and practical criterion for determining the near- and far-field boundary along the axis of the circular piston as a function of frequency. This criterion is validated through theoretical analysis and experimental measurements. Overall, the results show the influence of circular piston parameters on the SPL spatial distribution.

Keywords: sound pressure level (SPL); spatial characteristics; near-field; far-field; boundaries; criterion.



Copyright © 2025 The Author(s).
This work is licensed under the Creative Commons Attribution 4.0 International CC BY 4.0
(<https://creativecommons.org/licenses/by/4.0/>).

1. Introduction

The study of sound's spatial characteristics plays a critical role in numerous engineering and medical applications (STEFANOWSKA, ZIELIŃSKI, 2024). Over the years, extensive research has been conducted on sound propagation in different environments, such as water (VAN GEEL *et al.*, 2022) and air (ILIEV, ZHIVOMIROV, 2015; KUDRIASHOV, 2017).

Additionally, various experiments have explored sound produced by different sources, including unconventional ones (ÖZTÜRK, TIRYAKIOGLU, 2020).

To better understand the sound field generated by an acoustic transducer, its spatial characteristics must be examined using both conventional and innovative methods (KLIPPEL, BELLMAN, 2016; SHI *et al.*, 2022). In this context, the sound pressure p_a is the physical quantity (parameter) that provides the most detailed information about the structure of the sound field in the space.

Theoretical analysis indicates that the SPL near a circular piston is not uniformly distributed. In classical acoustics, two primary regions are distinguished

around an acoustic source: the near-field and far-field. A third region, known as the very near-field, is primarily the subject of research in vibration mechanics. In some references, the near-field is referred to as the Fresnel zone, while the far-field is called the Fraunhofer zone. Each zone has distinct formulas for determining the sound pressure p_a . This raises questions about the delineation of the boundaries defining various zones and the corresponding SPL variations within each zone. Equally crucial is pinpointing the moment at which the SPL stabilizes, ensuring accurate sound reproduction.

This paper builds upon the author's previous research (ILIEV, ZHIVOMIROV, 2015), which provided a theoretical overview of established mathematical techniques for calculating the SPL generated by a circular piston in both near-field and far-field conditions. Expanding on that foundation, this work proposes a unified framework to define the boundary between the near- and far-field zone of a circular piston.

Understanding the formation of the SPL spatial structure around the acoustic transducer enhances its

design and application precision, especially in monitoring and screening systems.

2. Background

As shown by KINSLER *et al.* (2000) the total acoustic pressure p_a generated by a circular piston at an arbitrary point A (Fig. 1) can be obtained using the well-known Huygens–Fresnel principle (also referred to as the Rayleigh integral):

$$p_{a(\text{entire})}(\theta, f, r, t) = j\rho_s f \nu_m \int_Q \frac{1}{l} e^{j(2\pi ft - \frac{2\pi fl}{c})} dQ, \quad (1)$$

where θ – elevation angle; f – frequency of the sound signal; r – distance between the circular piston and observation point A ; t – time; ρ_s – density of the medium; ν_m – deformation amplitude the transducer surface; Q – surface area of the circular piston; l – distance between the elementary section dQ and observation point A ; c – speed of sound in the medium.

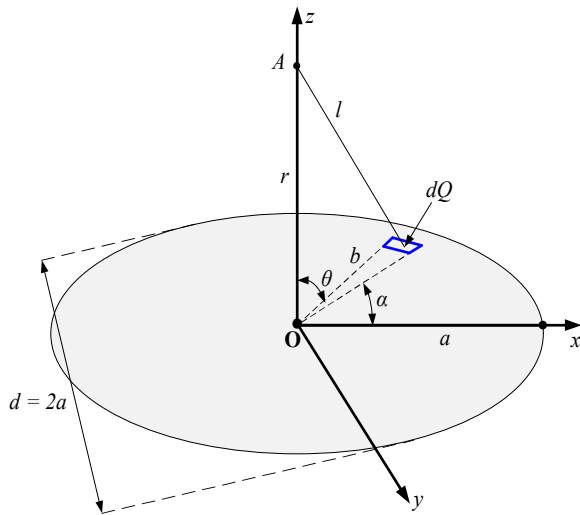


Fig. 1. Determination of the SPL in front of a circular piston.

Equation (1) is not suitable for direct practical implementation. However, the entire acoustic pressure $p_{a(\text{Entire})}$, generated by a circular piston, can also be computed using the authors' modified expression (ILIEV, 2014):

$$p_{a(\text{entire})}(\theta, f, r, t) = \rho_s f \nu_m e^{j2\pi ft} \int_0^a b db \int_0^{2\pi} \frac{e^{-\frac{j2\pi f}{c}(\sqrt{r^2+b^2+2rb\sin\theta\cos\alpha})}}{\sqrt{r^2+b^2+2rb\sin\theta\cos\alpha}} d\alpha, \quad (2)$$

where a – radius of the circular transducer; b – radial distance between the elementary section (point source) dQ and the center of the circular piston O ; α – directivity angle (azimuth).

A simplified solution of Eq. (2) allows for calculating the sound pressure in the far-field $p_{a(\text{far})}$ (when $r \gg d$) on the axis of the circular piston (when $\theta = 0$), as follows (KINSLER *et al.*, 2000):

$$p_{a(\text{far})}(0, f, r, t) = \frac{\rho_s f \nu_m}{r} e^{j2\pi ft} \cdot \int_0^a b db \int_0^{2\pi} e^{-\frac{j2\pi fr}{c}} d\alpha. \quad (3)$$

Also, a simplified version of Eq. (2) for the near-field SPL $p_{a(\text{near})}$, on the axis of the circular piston, is given (KINSLER *et al.*, 2000):

$$p_{a(\text{near})}(0, f, r) = 2\rho_s f \nu_m \cdot \left| \sin \left\{ \frac{\pi fr}{c} \left[\sqrt{1 + \left(\frac{a}{r}\right)^2} - 1 \right] \right\} \right|. \quad (4)$$

Equation (4) is graphically represented in Fig. 2, evaluated for various distances and frequencies for a circular piston with $a = 0.08$ m. This provides insight into the spatial structure of the near-field SPL.

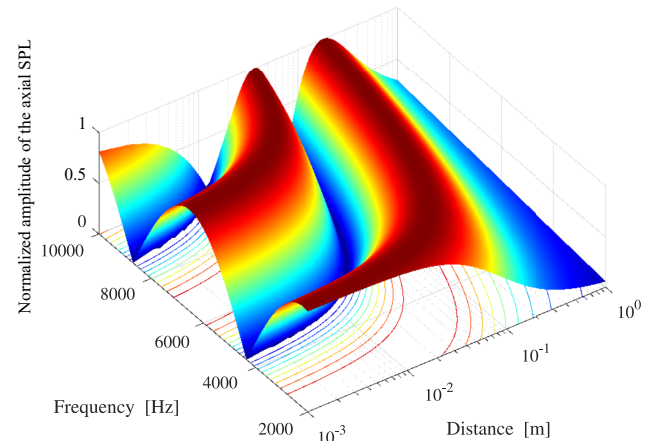


Fig. 2. Axial near-field SPL structure for various distances and frequencies for a circular piston with radius $a = 0.08$ m, evaluated by Eq. (4). The pulsations of the SPL are evident.

Equation (4) reveals that extrema in the axial SPL occur due to the sine function. For a constant sound speed c and a specific circular piston with radius a , the sine function reaches extremum values at distances (LEPENDIN, 1978):

$$r_m = \frac{a^2 f}{mc} - \frac{mc}{4f}, \quad (5)$$

where $m \in \mathbf{N}$. The maxima occur when m is odd, and the minima when m is even. The first SPL maximum (moving toward the circular piston axis) appears for $m = 1$, at a distance:

$$r_{\text{max(first)}} = \frac{a^2 f}{c} - \frac{c}{4f}. \quad (6)$$

This relationship is depicted in Fig. 3. It turns out that it represents the contour of the outer ridge of the SPL structure shown in Fig. 2.

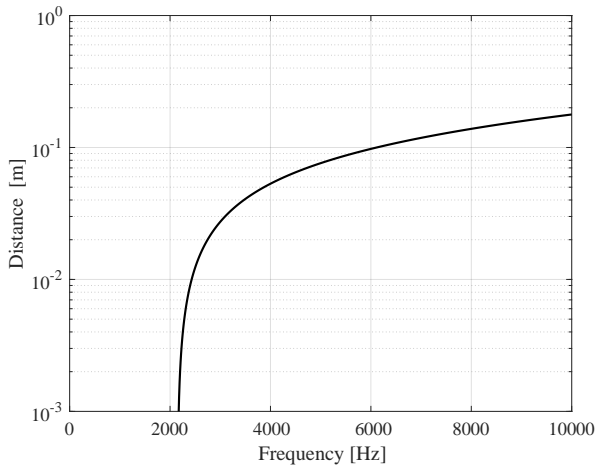


Fig. 3. Distance of the first axial SPL maximum, evaluated by Eq. (6), vs. frequency for a circular piston with $r = 0.08$ m. The plot can also address the problem of identification of the frequency of the first axial SPL maximum in relation to distance (see Eq. (7)).

For distances $r < r_{\max(\text{first})}$ the axial SPL suffers from maxima and minima, and for distances $r > r_{\max(\text{first})}$ the SPL decreases monotonically, approaching an asymptotic dependence $1/r$ (ROSSING, 2017). Therefore, one may consider the distance $r_{\max(\text{first})}$ as a reasonable threshold or dividing line between regions where the SPL is not completely formed and where the SPL becomes asymptotic. It is evident that r_m is frequency-dependent – the higher the frequency, the longer the near-field zone of the transducer.

Moreover, Eq. (6) reveals that the distance $r_{\max(\text{first})}$ has physical meaning only for frequencies $f > \frac{c}{2a}$ (ILIEV, 2014). For those frequencies, the radiation of the circular piston resembles that of a simple source, that is, without extrema.

Consequently, from Eq. (6), one can derive a relationship to determine the frequency of the first maximum:

$$f_{\max(\text{first})} = \frac{c(\sqrt{a^2 + r^2} + r)}{2a^2}. \quad (7)$$

It should be noted that different authors (KLEINER, 2013; GELFAND, 2017) have proposed various expressions (similar to Eq. (6)) to estimate the last maximum, which some consider the upper border distance of the near-field. In (KOZIEŃ, 2012), the hybrid intensity method is used to determine the boundary between the near and far fields. However, these methods have some disadvantages. The first (KLEINER, 2013; GELFAND, 2017) is too rough and lacks accuracy. The second method (KOZIEŃ, 2012) is too complicated and less practical.

Currently, there is no established criterion for delineating all zones, each with its unique characteristics, that influence the distribution and formation of the SPL in front of the circular piston.

3. Boundary between the near- and far-field

Identifying the region where sound pressure is fully developed provides valuable insights into the practical utility of a circular piston. Conversely, employing a circular piston at frequencies and distances where the SPL is not fully formed yields unsatisfactory outcomes.

In this paper, the authors introduce an enhanced method that not only determines the boundary between the fully developed acoustic field and the area where the acoustic field suffers from interferences, but also provide a new interpretation of the zones and their characteristics in front of the circular piston. The latter is based on the normalized difference between the axial SPLs calculated by Eqs. (2) and Eq. (3):

$$\Delta p_a(0, f, r) = \frac{p_{a(\text{entire})} - p_{a(\text{far})}}{p_{a(\text{far})}}. \quad (8)$$

For a given circular piston, the boundary can be identified in terms of distance and frequency when both Eq. (2) and Eq. (3) yield similar results.

The axial overall sound pressure level produced by a circular piston with a radius $a = 0.08$ m, as determined by Eq. (2), is shown in Fig. 4. Additionally, the axial far-field SPL, derived from Eq. (3), is depicted in Fig. 5. Both equations are numerically evaluated in the MathCAD environment and graphically represented in MATLAB[®]. The normalized difference between the entire field SPL and the far-field SPL on the axis, calculated by Eq. (8), is presented in Fig. 6.

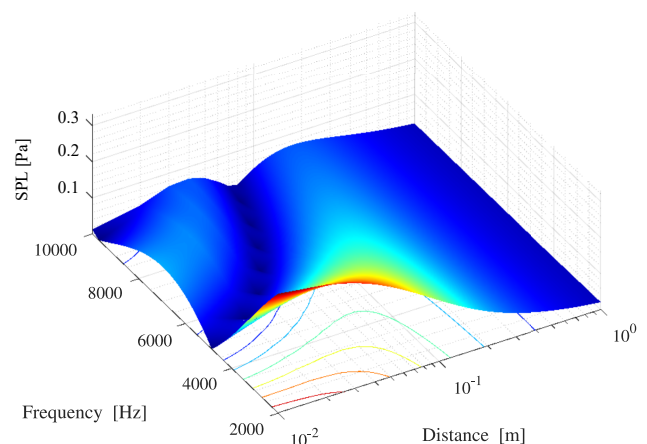


Fig. 4. Axial overall field SPL, evaluated by Eq. (2), for a circular piston with $r = 0.08$ m.

The authors propose that the distance where the SPL difference $\Delta p_a < 30\%$ (using the well-known 3 dB rule) should be considered the dividing line between the area with unstable SPL (i.e., the near-field zone)

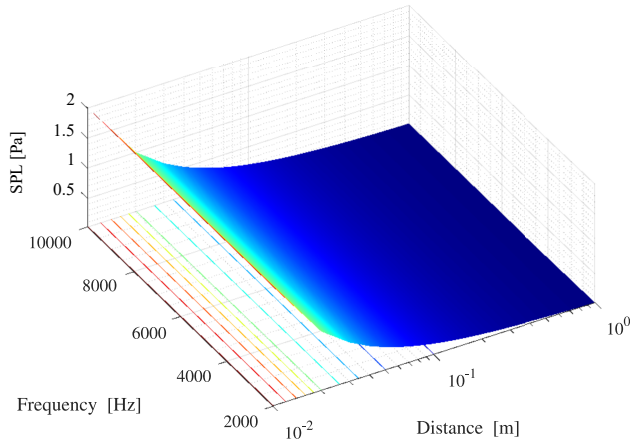


Fig. 5. Axial far-field SPL, evaluated by Eq. (3), for a circular piston with $r = 0.08$ m.

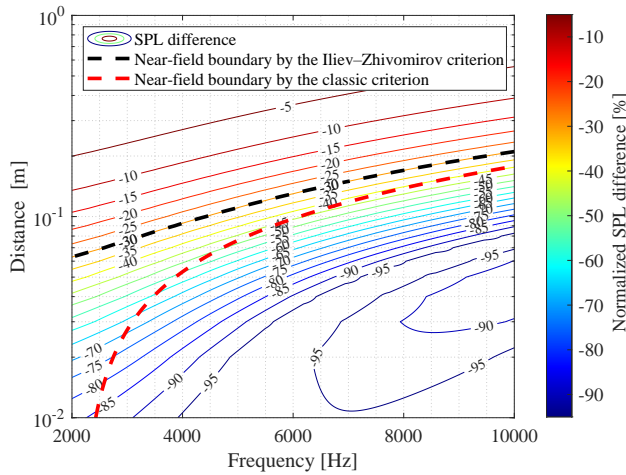


Fig. 6. Normalized SPL difference for a circular piston with $r = 0.08$ m, calculated by Eq. (8). The black dashed line depicts the boundary between the near- and far-field according to the newly proposed criterion. The red dashed line represents the outer ridge of the SPL structure, evaluated by Eq. (4).

and the area with asymptotic SPL (i.e., the far-field zone). It is evident that the boundary calculated by this rule strongly differs from the generally accepted rule-of-thumb, which is based on the outer ridge of the SPL structure evaluated by Eq. (4).

When applying the proposed method to distinguish the dividing line between the interferential area and the asymptotic area of the SPL for a circular piston with a radius $a = 0.08$ m, one observes interferences for frequencies $f > 2147$ Hz up the upper-frequency limit of the circular piston – 10 000 Hz. By applying the 30 % difference criterion between the SPLs calculated by Eq. (2) and Eq. (3), one can determine the distance r for each frequency where the SPL experiences interferences. For example, at $f = 5000$ Hz, using the isobars from Fig. 6, the interference region is found for $r < 0.11$ m (close to $r_{\max(\text{first})}$).

4. Experimental results

An experiment was conducted to validate the theoretical statements and provide a semi-quantitative, intuitive understanding of the proposed method, without claiming accuracy. In future work, more precise results will be obtained using numerical simulations and accurate measurements in a controlled environment.

The object of the experiment is a circular piston (loudspeaker) with a radius $a = 0.08$ m, identical to the loudspeaker with the same radius used for the theoretical analysis. For this loudspeaker, and taking into account the aforementioned factors, one may expect extremes in the SPL to occur between 2147 Hz and the maximum reproducible frequency of this loudspeaker model – 10 000 Hz.

Furthermore, for distances greater than $r > 0.065$ m at $f > 2147$ Hz and $r > 0.21$ m at $f = 10\,000$ Hz, the SPL is expected to decrease monotonically.

The measurements of the axial SPL are carried out using an active sound-level meter, DAQ-system, laptop, and MATLAB[®] software developed by the authors. The measurements are performed using a sine-wave signal with a frequency of $f = 5000$ Hz at eight different distances: $r = \{0.001, 0.01, 0.05, 0.1, 0.2, 0.3, 0.4, 0.5\}$ m. The results are shown in Fig. 7 and are compared with the theoretical axial SPL in the near-field, calculated by Eq. (4).

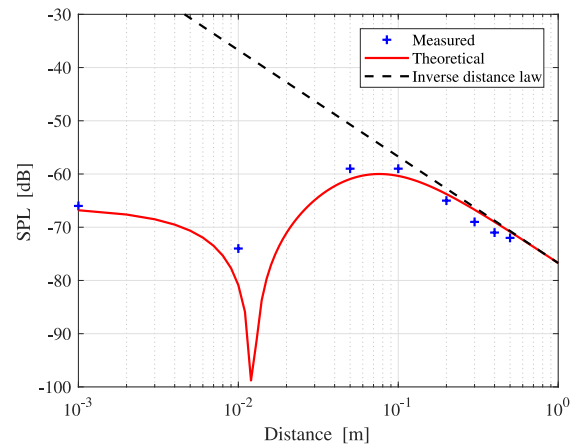


Fig. 7. Axial SPL at $f = 5000$ Hz theoretically estimated (solid red line) and measured at distances $r = \{0.001, 0.01, 0.05, 0.1, 0.2, 0.3, 0.4, 0.5\}$ m (blue crosses).

There is a well-pronounced overlap between the measured SPL (represented by blue crosses) and the predicted theoretical SPL (solid red line). Noticeable extrema in the axial SPL occur at $r = 0.012$ m (SPL minimum) and $r = 0.076$ m (SPL maximum), which are theoretically predicted by Eq. (5) for this particular operating frequency. For relatively large distances r , the theoretical and the experimental SPLs decrease monotonically, approaching an asymptotic dependence $1/r$ (black dashed line), in agreement with

Eqs. (3) and (4), and the proposed interpretation. In this particular case, the near-field boundary is situated at $r = 0.11$ m, according to Eq. (8). Beyond this point, the SPL decreases strictly monotonically, as expected.

5. Conclusion

The newly proposed method for distinguishing the dividing line between the interference and asymptotic areas of the SPL produced by a circular piston is relatively simple, easy to apply, and practically accurate. If one knows the radius a and frequency f of the circular piston, one can implement Eqs. (2), (3), and (8) to generate a graph similar to those shown in Fig. 6.

From the presented review of the different areas in front of the circular piston, the following conclusions can be drawn:

- the larger the circular piston radius a , the longer the interference area;
- the higher the frequency f , the longer the interference area;
- the higher the sound speed c , the shorter the interference area.

Furthermore, when dealing with complex signals exhibiting a complex and non-stationary spectral composition, a region of pronounced distortions in the sound field emerges within a specific area in front of the circular piston (specifically, between 0 m and 0.21 m in this case). This occurs due to the fact that for certain spectral components, this region functions as a near-field zone. In contrast, for others, it represents a far-field zone.

In this context, it becomes highly significant to define an “unconditional far-field zone”, which is determined by the maximum frequency of the considered signal or the maximum reproducible frequency of the circular piston, whichever is lower. Likewise, the concept of an “unconditional near-field zone” needs to be introduced, with its boundary defined by either the psychical characteristics of the circular piston ($f > \frac{c}{2a}$) or by the lowest frequency within the signal spectrum, whichever is higher. The intermediate region between these two zones can be referred to as the “transitory zone”.

The results shown in Figs. 2, 3, 4, 5, and 7 can be reproduced by the user using the MATLAB[®] scripts and data given in (Zhivomirov, Iliev, 2024) as supplementary material. This allows for a better understanding of the visualization and the ability to reuse or adapt the code for specific user data.

The conclusions drawn in this paper should be considered in the development of various screening systems (such as sonography, sound localization systems, audio systems, etc.) and in the development of systems using circular pistons in general.

References

1. GELFAND S.A. (2017), *Hearing: An Introduction to Psychological and Physiological Acoustics*, 6th ed., CRC Press, USA, <https://doi.org/10.1201/9781315154718>.
2. ILIEV I. (2014), Polar response of a circular piston, *TEM Journal*, **3**(3): 230–234.
3. ILIEV I., ZHIVOMIROV H. (2015), On the spatial characteristics of a circular piston, *Romanian Journal of Acoustics and Vibration Journal*, **12**: 29–34.
4. KINSLER L.E., FREY A.R., COPPER A.B., SANDERS J.V. (2000), *Fundamentals of Acoustics*, 4th ed., Wiley, USA.
5. KLEINER M. (2013), *Electroacoustics*, Taylor & Francis, USA, <https://doi.org/10.1201/b13859>.
6. KLIPPEL W., BELLMAN C. (2016), Holographic near-field measurement of loudspeaker directivity, *Journal of the Audio Engineering Society*, **141**: 9598.
7. KOZIEŃ M. (2012), Acoustic nearfield and farfield for vibrating piston in geometrical and intensity formulations, *Acta Physica Polonica A*, **121**: 132–135, <http://doi.org/10.12693/APhysPolA.121.A-132>.
8. KUDRIASHOV V. (2017), Improvement of range estimation with microphone array, *Journal of Cybernetics and Information Technologies*, **17**(1): 113–125, <https://doi.org/10.1515/cait-2017-0009>.
9. LEPENDIN L. (1978), *Acoustics* [in Russian], pp. 264–267, Graduate School, Moscow, USSR.
10. ÖZTÜRK H., TIRYAKIOĞLU B. (2020), Radiation of sound from a coaxial duct formed by a semi-infinite rigid outer cylinder and infinite inner cylinder having different linings, *Archives of Acoustics*, **45**(4): 655–662, <https://doi.org/10.24425/aoa.2020.135253>.
11. ROSSING T.D. (2017), *Handbook of Acoustics*, pp. 86–91, Springer, USA.
12. SHI T., BOLTON J.S., THOR W. (2022), Acoustic far-field prediction based on near-field measurements by using several different holography algorithms, *Journal of the Acoustical Society of America*, **151**(3): 2171–2180, <https://doi.org/10.1121/10.0009894>.
13. STEFANOWSKA A., ZIELIŃSKI S. (2024), Spatial sound and emotions: A literature survey on the relationship between spatially rendered audio and listeners’ affective responses, *INTL Journal of Electronics and Telecommunications*, **70**(2): 293–300, <https://doi.org/10.24425/ijet.2024.149544>.
14. van GEEL N.C.F., RISCH D., WITTICH A. (2022), A brief overview of current approaches for underwater sound analysis and reporting, *Marine Pollution Bulletin*, **178**: 113610, <https://doi.org/10.1016/j.marpolbul.2022.113610>.
15. ZHIVOMIROV H., ILIEV I. (2024), Mapping sound pressure level of a circular piston (supplementary material), Mendeley Data, V2, <https://doi.org/10.17632/b89rhwhrrk.2>.